Langmuir

Article

pubs.acs.org/Langmuir

Fabrication of Heterogeneous Double-Ring-Like Structure Arrays by Combination of Colloidal Lithography and Controllable Dewetting

Difu Zhu, He Huang, Gang Zhang, Xun Zhang, Xiao Li, Xuemin Zhang, Tieqiang Wang, and Bai Yang*

State Key Laboratory for Supramolecular Structure and Materials, College of Chemistry, Jilin University, Changchun 130012, P. R. China

Supporting Information

ABSTRACT: We report a novel technique for fabricating the heterogeneous double-ring-like structural array by colloidal lithography and two-step dewetting process. First, the 2D non-closed-packed (ncp) silica sphere arrays were obtained by lift-up lithography. Then, the ncp sphere array transferred onto the Rhodamine B (RB)@poly(vinyl alcohol) (PVA) film was used for the mask during reactive ion etching (RIE) process. Sequentially, the substrate with RB@PVA ring-like structure arrays under the silica sphere was dip-coated from poly(*N*-vinylcarbazole) (PVK) chloroform solution with certain concentration. Due to the presence of ordered 2D sphere arrays, the two-step dewetting behavior happened on top of the sphere and the silicon wafer between adjacent spheres, respectively. After removing the silica sphere arrays by hydrofluoric acid, the RB@PVA/PVK heterogeneous double-ring-like structure array was exhibited on the substrate. We characterized this particular structure by SEM, AFM, and fluorescence spectrum, which prove that both the inner RB@PVA ring and outer PVK ring are independent without any reaction. Accordingly, this method could be extended to other materials owing to its universality. These unique structural arrays have potential application in optoelectronic devices, surface photocatalysis, and surface enhanced Raman scattering (SERS).

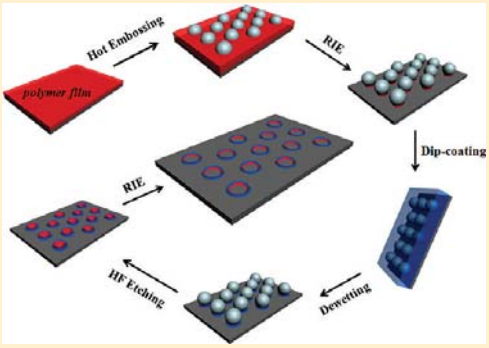

INTRODUCTION

The fabrication of submicrometer-sized rings has recently attracted the attention of scientists due to a general interest in shaping material into various geometries and due to several more subtle physical properties of rings in that size.[1−3] Rings made from metallic or superconducting materials can give rise to persistent currents if exposed to a magnetic field.[4−7] Rings exhibit tunable plasmon resonance in the near-infrared, and therefore might be used as elements in nonlinear optical devices and improved probes for surface enhanced Raman scattering.[8] Arrays of macroscopic metal rods and split rings can give rise to materials with a negative refractive index for radiation of appropriate wavelength.[7]

A variety of methods exist to create submicrometer-sized structures.[9−16] For example, photolithography provides a top-down method for fabricating large areas of well-defined features.[9] However, the capabilities of conventional photolithography are typically restricted to the diffraction limit of light (>100 nm). On the other hand, electron-beam lithography (EBL) is able to create features of two-dimensional (2D) geometry on a scale below 100 nm.[10] Despite its high resolution, EBL is time-consuming when large arrays are required. Moreover, the process must take place at a dedicated facility in a vacuum environment with relatively expensive equipment. These restrictions have motivated the search for alternative pathways to fabricating large areas of ordered patterns.[17−19] The colloidal sphere lithography attracted attentions for successful fabrication of ordered nanostructures over large areas.[20−24] In this process, the latex particles self-organized into ordered pattern first, and then 2D array was obtain by depositing the desired material onto the ordered colloidal.[25−33] Several methods were suitable for the colloid monolayer, such as Langmuir−Blodgett,[34] spin-coating,[35−37] and self-assembly method.[38,39]

Recently, our research group has developed a lift-up and transfer-printing method to fabricate 2D ncp colloidal microsphere arrays.[40] PDMS elastomeric stamps were used to lift up 2D self-assembled close-packed colloidal crystal arrays, and then deformed by solvent swelling or mechanical stretching to adjust the lattice structures of 2D arrays of microspheres. Using this method, we can tune the interparticle distance or change the lattice structure of the 2D ncp colloidal crystals. Moreover, in our past work, ordered submicrometer ring arrays were fabricated by controllable dewetting process simply.[41] On the physically heterogeneous surfaces, raised place (such as water droplet or colloidal sphere) could induce dewetting behavior due to defects nucleation mechanism.[42]

In this paper, we combined colloidal sphere lithography with controllable dewetting process. First, the 2D ncp colloidal sphere arrays were fabricated by lift-up and transfer-printing

Received: September 11, 2011
Revised: December 15, 2011
Published: January 3, 2012

dx.doi.org/10.1021/la203558b | *Langmuir* 2012, 28, 2873−2880

method. Then, using this sphere arrays as mask, Rhodamine B (RB)@poly(vinyl alcohol) (PVA) ring-like structure arrays were formed by RIE process. From experimental process, we found that colloidal spheres play an important role in the whole operation, since that they serve as not only a template in the formation of ring arrays, but also the "defect" in the controllable dewetting process. Therefore, the poly(*N*-vinylcarbazole) (PVK) ring-like structures were fabricated outside the RB@PVA rings through controllable dewetting. Finally, after removing the colloidal spheres, the heterogeneous RB@PVA/PVK double-ring-like structure arrays were obtained. As a result of the universality of this method, ordered large-area heterogeneous structure arrays could be fabricated, as long as these two materials are not miscible, or could not react with each other. These unique structure arrays have potential application in optoelectronics device, data storage, surface photocatalytic, and surface-enhanced Raman scattering (SERS).

EXPERIMENTAL SECTION

Materials. Monodispersed silica spheres (500 nm) were prepared in ethanol according to the Stöber method.[43] A drop of 10−20 μL of colloidal suspension was applied to the slightly tilted substrate to form colloidal crystals with control over temperature and ambient humidity. Silicon (100) wafers were cleaned by immersion into a solution of H_2SO_4/H_2O_2 (v/v, 7/3) for about 5 h at 90 °C, and then rinsed with a large amount of distilled water and dried by nitrogen gas. Poly(dimethylsiloxane) (PDMS) elastomer kits (Sylgard 184) were purchased from Dow Corning (Midland, MI). Poly(*N*-vinylcarbazole) (PVK, M_w = 90 000) and trichloro (1*H*,1*H*,2*H*,2*H*-perfluorooctyl) silane (PFS) were purchased form Aldrich. Hydrofluoric acid, sulfuric acid, hydrogen peroxide, poly(vinyl alcohol) (PVA, M_w = 71 000), Rhodamine B ($C_{28}H_{31}ClN_2O_3$, M_w = 479.0175), and ethanol were used as received.

Characterization. Scanning electron microscopy (SEM) images were made on a JEOL JSM6700F field emission scanning electron microscope with primary electron energy of 3 kV. Atomic force microscopy (AFM) image was measured with Digital Instruments NanoScope IIIa in tapping mode. Thickness of polymer film was measured by Veeco dektak150 surface profiler. The optical and fluorescent images were recorded on an Olympus BX51 microscope (in reflection mode) and were captured with a MVC1000 USB2.0 megapixel camera.

Fabrication of ncp Colloidal Sphere Arrays on Rhodamine B@PVA Film. A schematic illustration of the experimental procedure is shown in Scheme 1. Briefly, 1−8 wt % aqueous solution of PVA (containing 2 mM Rhodamine B) were spin-coated on a silica substrate at a spinning speed of 3000 rpm and a spinning time of 60 s respectively. Subsequently, the PDMS stamp was brought into conformal contact with the colloidal film and hot-pressed. By utilizing the lift-up method previously reported, 2D hexagonal close-packed colloidal microsphere arrays were transferred onto the surface of PDMS.[44] After a deformation of PDMS swelled by immersion into toluene for 5 min, close-packed microsphere arrays became non-close-packed arrays, and then were transferred onto the surface of RB@PVA film using a modified microcontact printing. After heating at 180 °C for 2 h, the silicon microspheres were embedded into the RB@PVA film. These ncp colloidal sphere arrays were used in colloidal lithography as masks for reactive ion etching (RIE).

Fabrication of Rhodamine B@PVA Ring-Like Structure Arrays. The RIE process was using for removing the RB@PVA film without mask shading. For the RIE process, the oxygen plasma was delivered by a commercially available etching machine (Oxford Plasmalab 80 Plus RIE) including an inductively coupled plasma (ICP) source. The following plasma parameters were applied: O_2, 50 sccm; ICP power, 300 W; RF power, 30 W; total pressure, 10 mTorr (1 Torr = 133.3 Pa); nominal substrate temperature, 20 °C. The RIE process was performed as described above for 30 s.

Scheme 1. Diagrammatic Sketch of the Procedure for Fabrication of Ordered Heterogeneous Double-Ring-Like Structures Arrays by Combination Colloidal Lithography with Controllable Dewetting on the Silica Substrate

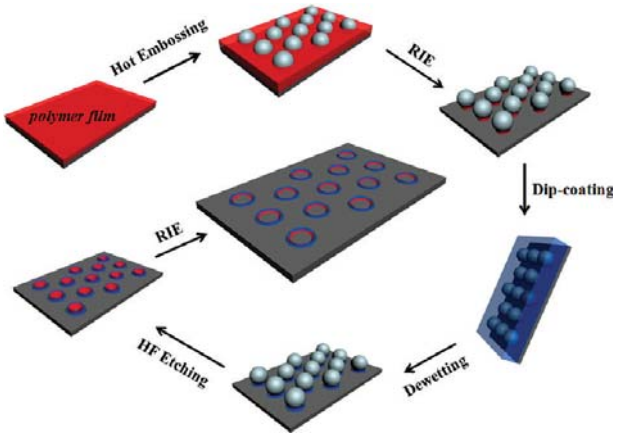

Fabrication of Rhodamine B@PVA/PVK Heterogeneous Double-Ring-Like Structure Arrays. The substrate with RB@PVA ring-like structures under the sphere arrays was placed in a sealed vessel, on the bottom of which was dispensed a few drops of PFS. There was no direct contact between the substrate and the drops. The vessel was put in an oven at 80 °C for 6 h to enable the vapor of PFS to react with the OH groups on the exposed surface. Then, the substrates were dipped into PVK chloroform solutions with different concentrations (0.1, 0.5, and 2.0 mg mL^{-1}, respectively) and withdrawn immediately. With the complete evaporation of chloroform, ordered PVK ring-like structure arrays were obtained outside the RB@PVA ring arrays. Finally, the substrate was immersed into hydrofluoric acid (6%) to dissolve the silica microspheres, and RB@PVA/PVK double-ring-like structure arrays were obtained. By further RIE process, redundant polymers were removed between the adjacent rings and in the middle of every ring.

RESULTS AND DISCUSSION

Fabrication of ncp Colloidal Sphere Arrays. By using the lift-up soft lithography we reported,[44] 2D ncp silicon sphere arrays were achieved on the RB@PVA film. Figure 1a shows the SEM images of 2D hexagonal ncp silica spheres with average diameter (D) of 500 nm fabricated by swelling of the PDMS film with pure toluene. From this figure, we could observe the lattice spacing of the obtained crystal structure was extended to about 1.49 D, while the highly ordered hexagonal arrangement was preserved. Figure 1b shows the SEM image of the quasi-one-dimensional parallel wires of silica spheres that were fabricated by stretching the PDMS film along x-axis while maintaining the length of y-axis and the inset is a diagrammatic sketch of the stretching process. These wires were assembled by spheres touching each other along the y-axis and separated along the x-axis by about 1.41 D.

In RIE process, as the lattice structure of colloidal crystals is, the thickness of RB@PVA film is another influencing factor. The RB@PVA films with different thicknesses were introduced in our experiment. These films included 30−200 nm thicknesses obtained by spin-coating the RB/PVA hybrid aqueous solutions with different concentrations, as shown in Figure 2a. Subsequently, the 2D hexagonal ncp silica sphere arrays were transferred onto the RB@PVA films by a hot pressing process. When the thickness of RB@PVA film was 30 nm (from 1 wt % aqueous solution), we found silica sphere

dx.doi.org/10.1021/la203558b | *Langmuir* 2012, 28, 2873−2880

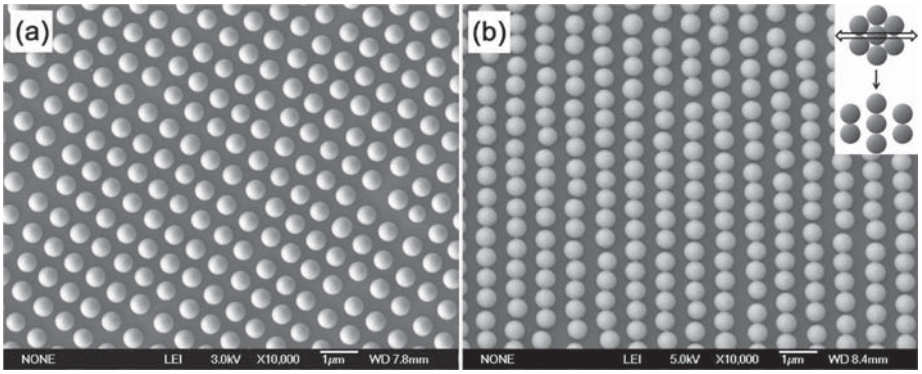

Figure 1. (a) SEM image of 2D hexagonal ncp silica spheres with average diameter of 500 nm fabricated by swelling of the PDMS film with pure toluene. (b) SEM image of silica spheres with average diameter of 500 nm fabricated by stretching. The inset of (b) is a diagrammatic sketch of the stretching process.

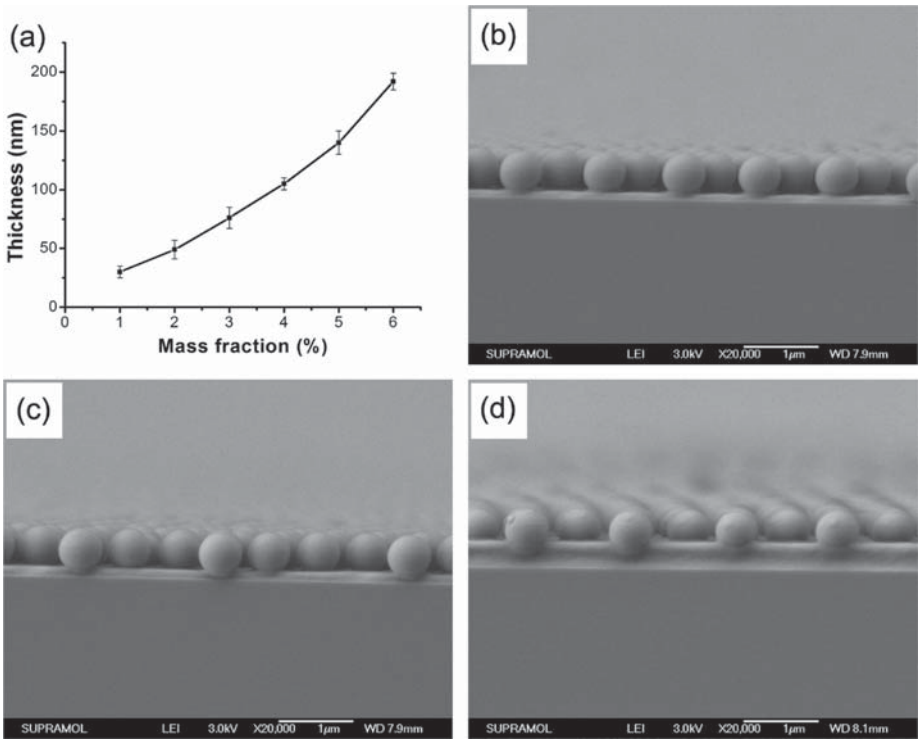

Figure 2. (a) Relationship curve between the mass fraction of RB@PVA solution and the average thicknesses of the films which were produced from the same experimental conditions at 3000 rpm. (b–d) Colloidal spheres partially embedded in the RB@PVA films with different thicknesses: (a) 2%, 50 nm; (b) 4%, 110 nm; (c) 8%, 700 nm.

arrays could not be transferred on the substrate at all. In this condition, after annealing process, the contact area between silica sphere and RB@PVA film was rather small. The interaction forces between silica sphere and RB@PVA film were weaker than that between silica sphere and PDMS film. Therefore, the silica sphere arrays remained on the PDMS film instead of transferring onto RB@PVA film. In addition, when using the PVA solution with 2 wt % or higher concentration, the silica sphere arrays could be transferred onto the RB@PVA films completely. In the section image, we could observe that silica spheres were embedded into RB@PVA films, the thickness of which were about 50 nm (Figure 2b) and 110 nm (Figure 2c), and nearly in contact with the silicon substrate. In further experiments, when the concentration increased to 6 wt % (film thickness was about 200 nm), there was still polymer film between silica spheres and silicon substrate after the hot pressing process. Figure 2d shows the silica spheres were embedded into RB@PVA film, the thickness of which was 500 nm. In this image, 2/5 of the sphere fell into PVA film, and the distance between spheres and substrate was 300 nm.

Fabrication of Rhodamine B@PVA Ring-Like Structure Arrays. In comparison with the closed-packed colloidal sphere arrays, ncp arrays had particular advantages in the RIE process. As a result of the space between adjacent spheres of ncp arrays, the RB@PVA film exposed to reactive ion bombardment was etched away easily. By adjusting the etching period, the ring-like structure arrays could be fabricated under the sphere arrays. Predictably, if the closed-packed colloidal sphere arrays were

dx.doi.org/10.1021/la203558b | *Langmuir* 2012, 28, 2873–2880

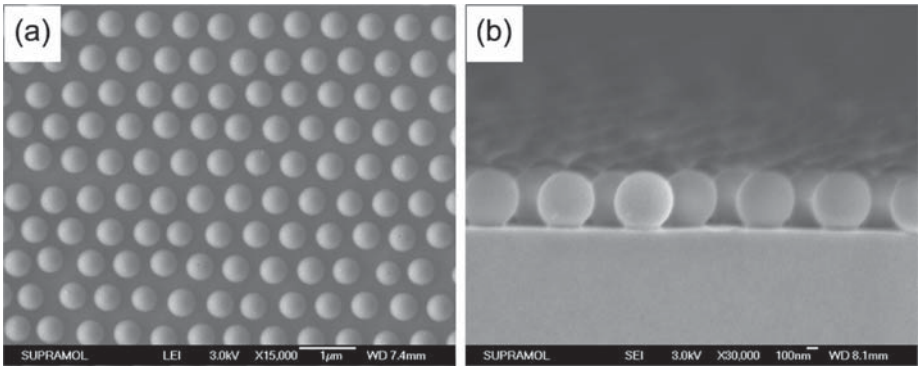

Figure 3. SEM images of RB@PVA ring-like structure array before removing the sphere arrays: (a) top view and (b) sectional view.

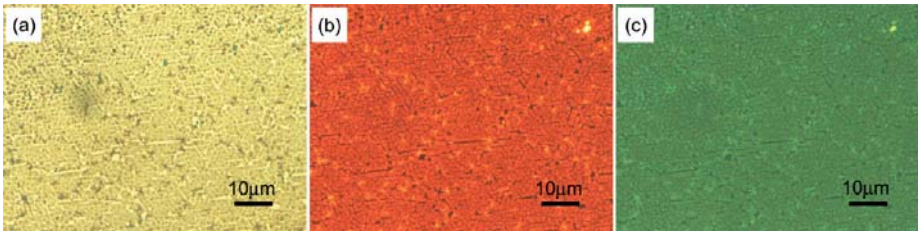

Figure 4. Optical image (a) and fluorescent images (b and c) of RB@PVA ring-like structure arrays on silicon substrate. The image (b) is captured under green light excitation and (c) is captured under UV excitation.

used for a mask, grid structures would be obtained instead of ring arrays. Figure 3 shows the SEM images of RB@PVA film under the mask of ncp hexagonal silica sphere arrays after RIE process (the thickness of the polymer is 50 nm and the etching period is 30 s). From the top view, we could observe that the dimension of spheres did not decrease, and the crystal lattice was not damaged. It is proven that the ncp silica sphere arrays could serve as an excellent mask in the RIE process. In the section image, we found that the RB@PVA thin films were fabricated under the silica sphere, and no polymer residue was observed between adjacent spheres on the substrate. After removing silica sphere arrays by hydrofluoric acid, the RB@PVA ring-like structure arrays were exposed on the substrate. Figure 4a is an optical micrograph of the regular arrays of RB@PVA ring-like structures formed on the silica substrate. Figure 4b and c shows the fluorescent images of a large area of 2D ordered RB@PVA ring-like structure arrays, which exhibit intensive red luminescence by the excitation of a green emission source in Figure 4b and green luminescence under ultraviolet (UV) in Figure 4c. These images show the regular arrays and fine fluorescence, which prove that the properties of RB@PVA ring-like structures are not influenced by hot pressing, RIE process, or hydrofluoric acid washing. Since the PVA films serve as a supporter here, a variety of materials could be introduced to this system, such as magnetic nanoparticles.

During the experiment, we found that the morphology of the RB@PVA ring-like structure is influenced by the film thickness and the etching period. With one of them fixed, the different morphologies would be obtained by changing the other. It is conceivable that these two conditions are essentially the same, which means that the thicker film requires a longer period to etch off. Here, an etching period of 30 s was employed in the experiment. The 50-nm-thickness film (from 2 wt % PVA aqueous solution) and 150-nm-thickness film (from 5 wt % solution) were used for the RIE process. After etching for 30 s, two kinds of ring-like structure arrays with different morphologies were obtained, as shown in Figure 5. From the

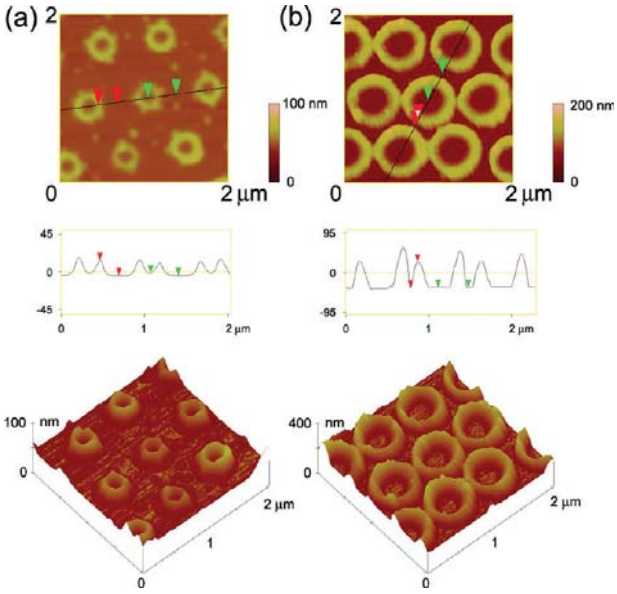

Figure 5. The height mode AFM images, corresponding cross-sectional analysis images, and 3D images of ring-like structure array by RIE for 30 s fabricated from (a) 50 nm and (b) 150 nm RB@PVA films.

height-mode AFM images, we could observe that the arrays are arranged hexagonally as the silica sphere array mask. In the corresponding cross-sectional analysis of Figure 5a, the rings are on average 20 nm in height, 120 nm in width, and 300 nm in diameter. Compared with the condition before RIE process, the height of the ring was lower than the thickness of PVA film

dx.doi.org/10.1021/la203558b | *Langmuir* 2012, 28, 2873–2880

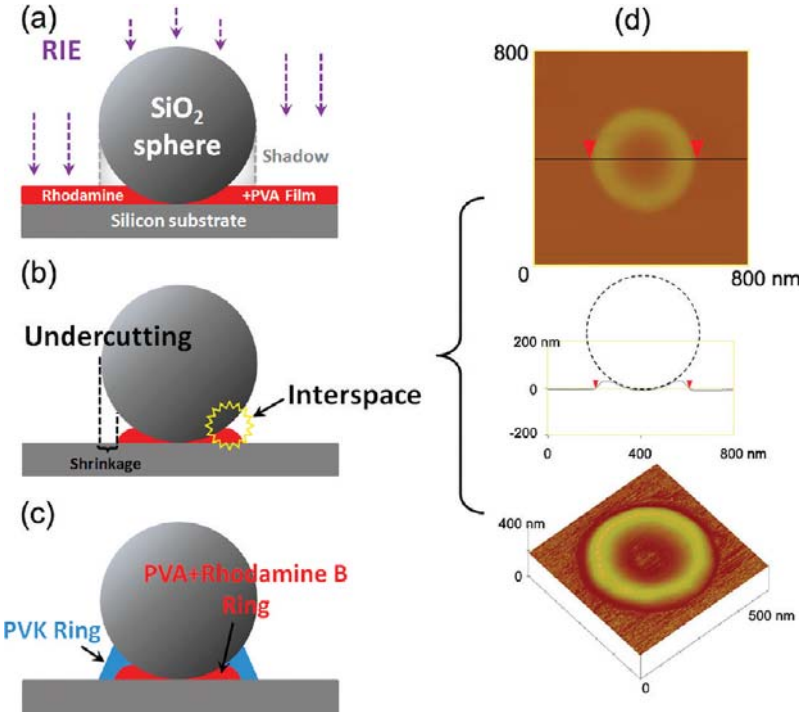

Figure 6. (a–c) Sectional schematic diagram of the formation of heterogeneous double-ring-like structure from thin film. (d) Height mode AFM images, corresponding cross-sectional analysis images, and 3D images of ring-like structure by RIE process.

(50 nm), and the outer diameter of the ring was smaller than the diameter of the silica spheres (500 nm). In Figure 5b, we could observe that the rings are on average 80 nm in height, 175 nm in width, and 600 nm in diameter. Correspondingly, the height of the ring was lower than the thickness of PVA film (150 nm) before etching, but the outer diameter of the ring was larger than that of the silica spheres.

Investigation of Ring-Like Structure Formation in the RIE Process. For polymer films with different thickness, the morphologies of ring-like structure arrays would vary after RIE process, as shown in Figure 5. We divided the relationship between thickness of polymer film (H) and radius of silica sphere (R) into three conditions: $H < R$, $H \approx R$, and $H > R$. Figure 6 is the schematic diagram of ring-like structure formation under the silica sphere in the RIE process (when the condition is $H < R$). First, silica spheres were embedded into the polymer film by the hot pressing process; meanwhile, a "shadow" formed under the sphere (Figure 6a). During RIE process, the films under "shadow" were protected by silica sphere, and the other films exposed to the RIE were eliminated. Furthermore, due to the undercutting or excessive etching in process, the outer diameter of the ring-like structure could be smaller than the diameter of the silica sphere, and a space appeared between the sphere and the RB@PVA ring-like structure on the substrate (Figure 6b). Here, the interspace would be used for fabrication of the outer PVK rings in a further operation, which was benefit from capillary force. Sequentially, the heterogeneous double-ring-like structure would be obtained by two-step controllable dewetting (Figure 6c). The detail of outer PVK ring array formation will be discussed in the next part. Figure 6d shows a series of AFM images of RB@PVA ring-like structures in this condition. From these images, we observe that the average diameter of the rings is about 300 nm, which is smaller than the diameter of the silica spheres (500 nm).

When the condition is $H \approx R$, there is no "shadow" appearing between the sphere and the substrate. However, when the annealing temperature is above the glass transition temperature (T_g) in the hot pressing process, dewetting of the polymer film takes place on the substrate, so that a crater-like structure would form around the silica sphere (Figure 7a). After

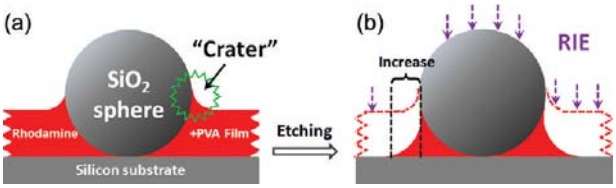

Figure 7. Sectional schematic diagram of the ring-like structure formation from thick film.

RIE process (etching period is 30 s), the films between two adjacent spheres were also etched off as in the condition mentioned above ($H < R$). By contrast, the outer diameter of the ring-like structure here was larger than the diameter of the sphere, as a result of the existence of the crater (Figure 7b). In this morphology, there was no space to fabricate the outer ring in a further operation. It is worth pointing out that the outer dimensions of the ring-like structure would continue to shrink with the increase of etching period owing to "undercutting".[45] For the condition $H > R$, due to the sphere arrays not in contact with the substrate, the ring-like structure would not be obtained after RIE process.

Influence of the Lattice Structure of Colloidal Sphere Mask. In the experiment above, the mask with 2D hexagonal

dx.doi.org/10.1021/la203558b | *Langmuir* 2012, 28, 2873–2880

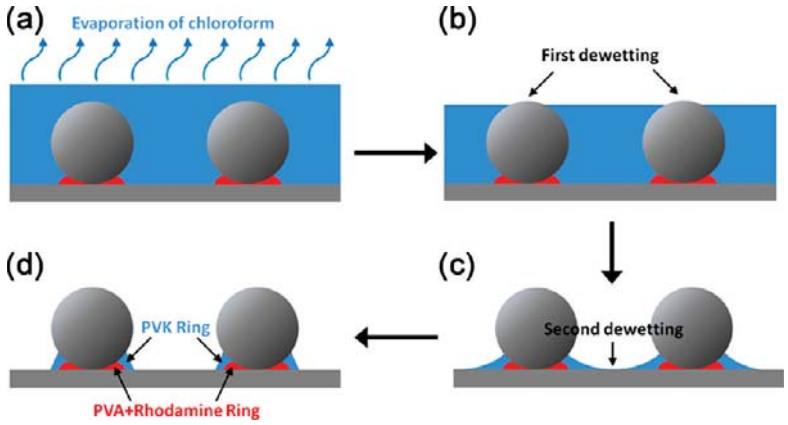

Figure 8. Schematic drawing of two-step controllable dewetting process. The first dewetting happened on top of the spheres, and the second took place on the silica substrate.

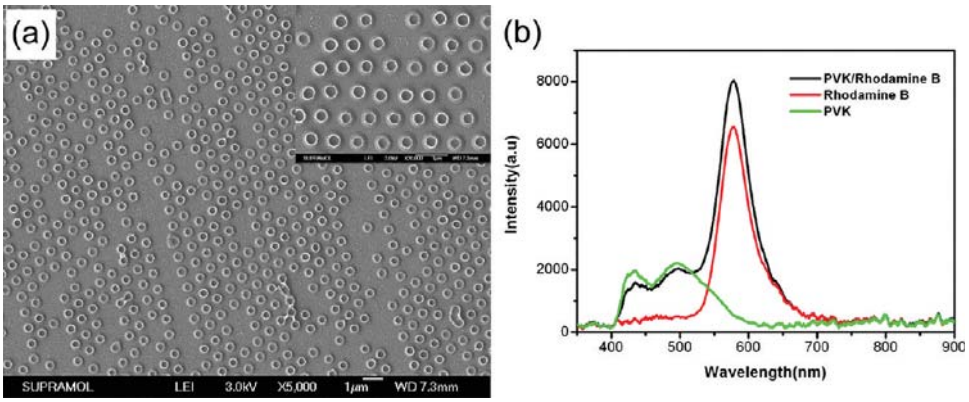

Figure 9. (a) SEM image of RB@PVA/PVK double-ring-like structure from the concentrations of PVK solutions 0.1 mg mL^{-1}. (b) Photoluminescence (PL) spectra of PVK ring-like arrays, RB@PVA ring-like arrays, and RB@PVA/PVK double-ring-like arrays.

ncp silica sphere arrays was prepared by swelling the PDMS stamp. On the other hand, when stretching the colloidal crystal-loaded PDMS sheet, the lattice structure could be changed due to anisotropic deformation. The quasi-one-dimensional parallel wires of silica spheres were obtained by stretching in single direction, as shown in Figure 1a. Using this mask for the RIE process, chain-like structures were fabricated, as shown in Supporting Information Figure 1. From these images, we could observe that the adjacent polymer rings connect with each other along the chain direction, and the polymer films between neighboring chains were etching off. In our previous work, 2D ncp colloidal crystal with Bravais lattice structures and controllable lattice features could be obtained by combining a circular lift-up process and modified soft lithography technique.[40] In this case, the diverse arrangement of ring-like structure arrays would be fabricated simply.

Fabrication of Heterogeneous Rhodamine B@PVA/PVK Double-Ring-Like Structure Arrays. Figure 8 is the schematic drawing of a two-step controllable dewetting process on the substrate with ordered silica sphere arrays. During dip coating, a liquid film of chloroform solution was initially deposited on the substrate-covering spheres, and then the liquid film became unstable as it was thinned by the evaporation of chloroform (Figure 8a). With the decline of the liquid surface, first dewetting took place due to heterogeneous nucleation (initiated by top of sphere), as shown in Figure 8b. When the liquid film was thinned below a critical thickness by further evaporation of chloroform, second dewetting would happen on the surface of the silicon wafer owing to the capillary force between the sphere and the substrate (Figure 8c). Next, with the complete evaporation of chloroform, the PVK rings were fabricated around the RB@PVA ring-like structure under the sphere (Figure 8d). Finally, after removing the silica sphere by hydrofluoric acid washing, the heterogeneous RB@PVA/PVK double-ring-like structure arrays were exhibited. Figure 9a is the SEM image of heterogeneous RB@PVA/PVK double-ring-like structure arrays. We could observe that the morphology of the double-ring-like structures is quite uniform in the inset of Figure 9a. Figure 9b is photoluminescence (PL) spectra of RB@PVA ring-like structure arrays, PVK ring arrays, and the heterogeneous RB@PVA/PVK double-ring-like structure arrays. Here, PVK showed blue-green PL with two peaks at around 434 and 494 nm. RB@PVA showed orange-red PL with a peak at around 578 nm. The fluorescent RB@PVA/PVK double-ring-like structure arrays yield a distinct multipeak spectrum, correlating well with the composition of two fluorescent materials, and the peaks match the original PL spectra well with negligible shifts. It is considered that the formation of heterogeneous double-ring-like structure arrays did not affect their respective luminescent properties by this strategy.

Influence of Concentration of the PVK Solution. In our previous work,[46] the morphology of the ordered ring array was influenced by the concentration of the polymer solution

dx.doi.org/10.1021/la203558b | *Langmuir* 2012, 28, 2873–2880

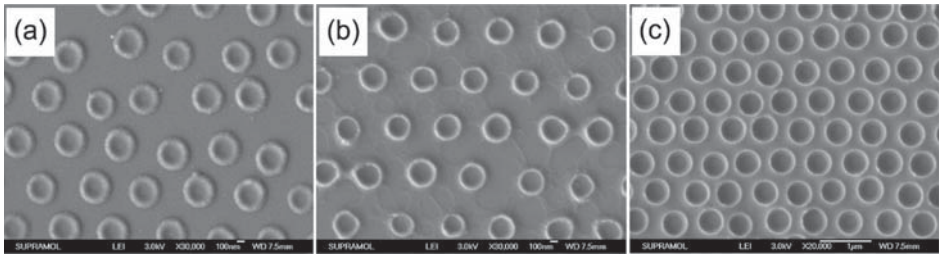

Figure 10. SEM images of various morphologies of RB@PVA/PVK heterogeneous structures from different concentrations of PVK solutions (a) 0.1 mg mL^{-1}, (b) 1 mg mL^{-1}, and (c) 5 mg mL^{-1}.

through the controllable dewetting process. Here, we found that the morphology of the ring-like structure was also dependent on the concentration of PVK coating solution. Figure 10 shows the SEM images of a series of samples produced by using 0.1, 1.0, and 5.0 mg mL^{-1} PVK chloroform solutions, respectively. From Figure 10a, we observed that the PVK ring-like structure array had been obtained by dip-coating in 0.1 mg mL^{-1} PVK solution. However, under the concentration conditions 1.0 and 5.0 mg mL^{-1}, grid structure (Figure 10b) and porous PVK film (Figure 10c) were obtained on the RB@PVA ring-like structure arrays instead of the ring array, respectively. We found that 4.0 mg mL^{-1} was the critical concentration for formation of the ring arrays. Above this concentration, porous PVK film could be formed on the RB@PVA ring-like structure arrays. In order to prove that the RB@PVA ring-like structure arrays were not damaged in the dewetting process, the porous PVK film obtained from 5.0 mg mL^{-1} PVK solution was inverted by washing in warm deionized water, as shown in Supporting Information Figure 2. From the SEM image of the top surface (Supporting Information Figure 2b), we could observe that crater-like structures were formed after removing the silica sphere. In the bottom surface image (Supporting Information Figure 2c), it is observed that ring-like grooves formed under the bottom of micropore, as a result of the RB@PVA ring being dissolved by warm water. These demonstrated that the heterogeneous structure had been successfully fabricated by our strategy and these two-part structures were mutually independent.

Atomic force microscopy could also help us prove the fabrication of outer PVK ring arrays. Figure 11a gives an AFM image of RB@PVA/PVK double-ring-like structure arrays, and the cross-sectional analysis image shows that the double-rings are on average 45 nm in height, 150 nm in width, and 540 nm in outer diameter. Compared with the corresponding RB@PVA ring-like structure arrays (shown in Figure 4a), the sizes of the features of double ring arrays are all larger than that of single ring arrays. These confirmed that the RB@PVA/PVK double-ring-like structure arrays were fabricated successfully in the topography. From Figure 11a, we found that the profile of the double-ring-like structure was not distinct and there were some residuals left on the substrate. In order to clean the substrate and make the structure regular, the substrate with RB@PVA/PVK double-ring-like structure arrays was treated by mild RIE process. Figure 11b shows the double-ring structure arrays after RIE process for 10 s. In these AFM images, the double-rings are on average 35 nm in height, 115 nm in width, and 465 nm in outer diameter. Compared to the array before etching, the contour profiles of rings become obvious and the residuals were eliminated entirely.

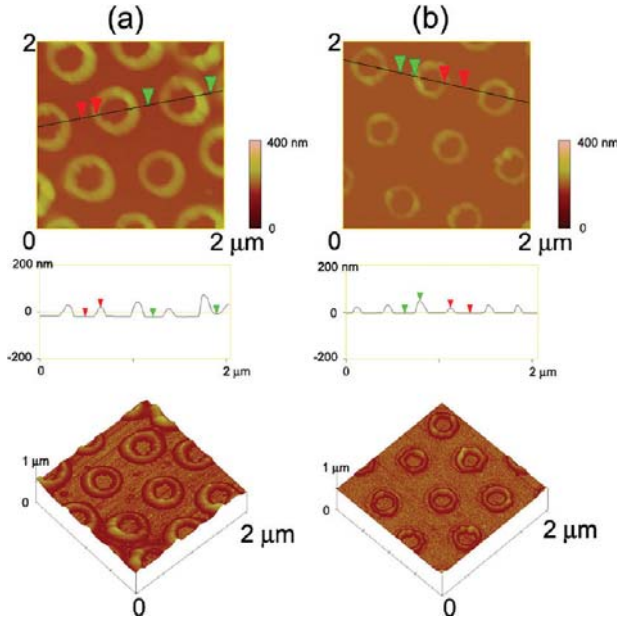

Figure 11. Height mode AFM images, corresponding cross-sectional analysis images, and 3D images of RB@PVA/PVK double-ring-like structure arrays (a) before and (b) after RIE etching.

CONCLUSION

In summary, the ordered RB@PVA/PVK heterogeneous double-ring-like structure arrays were fabricated via combining colloidal lithography technology with two-step dewetting process. Due to the swelling property of the PDMS elastomer, ncp silica colloidal sphere arrays were obtained. By the hot pressing method, the ncp sphere array was transferred onto the prepared RB@PVA film; moreover, the sphere array was partially embedded in the film and in contact with the substrate. Through the RIE process by the microsphere array mask, the RB@PVA ring-like structure array was formed under the sphere array. The morphology of the ring-like structures was influenced by thickness of the polymer film and etching period. Finally, the substrate with sphere arrays and ring-like structure arrays was dipped into the PVK chloroform solution. With chloroform volatilization, the two-step dewetting process happened on top of the spheres and the substrate surface, respectively. Following this, the PVK ring was fabricated around the RB@PVA ring. After further RIE etching, the ordered heterogeneous RB@PVA/PVK double-ring-like structure array was constructed successfully. These unique structure arrays have potential application in optoelectronics devices, data storage, surface photocatalysis, and surface enhanced Raman

dx.doi.org/10.1021/la203558b | *Langmuir* 2012, 28, 2873−2880

scattering (SERS). In addition, due to its universality, this method could be extended to other materials.

■ ASSOCIATED CONTENT

Supporting Information

AFM images of chain-like structure arrays and SEM images of porous PVK films.This material is available free of charge via the Internet at http://pubs.acs.org.

■ AUTHOR INFORMATION

Corresponding Author

*E-mail: byangchem@jlu.edu.cn.

■ ACKNOWLEDGMENTS

This work was supported by the National Natural Science Foundation of China (Grant No. 20534040, 20874039, 50703015, 51073070) and the National Basic Research Program of China (2007CB936402).

■ REFERENCES

(1) Manoharan, V.; Elsesser, M.; Pine, D. *Science* **2003**, *301*, 483.
(2) Jiang, P.; Bertone, J.; Colvin, V. *Science* **2001**, *291*, 453.
(3) Veliko, K.; van Dillen, T.; Polman, A.; van Blaaderen, A. *Appl. Phys. Lett.* **2002**, *81*, 838.
(4) Matveev, K.; Larkin, A.; Glazman, L. *Phys. Rev. Lett.* **2002**, *89*, 096802.
(5) Rabaud, W.; Saminadayar, L.; Mailly, D.; Hasselbach, K.; Benoit, A.; Etienne, B. *Phys. Rev. Lett.* **2001**, *86*, 3124.
(6) Levy, L.; Dolan, G.; Dunsmuir., J.; Bouchiat, H. *Phys. Rev. Lett.* **1990**, *64*, 2074.
(7) Smith, D.; Padills, W.; Vier, D.; Nemat-Nasser, S.; Schultz, S. *Phys. Rev. Lett.* **2000**, *84*, 4184.
(8) Aizpurua, J.; Hanarp, P.; Sutherland, D.; Käll, M.; Bryant, G.; Garcia de Abajo, F. *Phys. Rev. Lett.* **2003**, *90*, 057401.
(9) Moreau, W. *Semiconductor Lithography: Principles, Practices, and Materials*; Plenum: New York, 1989; Chapter 8.
(10) Sze, S. *VLSI Technology*; McGraw-Hill: Singapore; 1988; Chapter 4.3.
(11) Dändliker, R.; Gray, S.; Clube, F.; Herzig, H.; Vökel, R. *Microelectron. Eng.* **1995**, *27*, 205.
(12) Gale, M.; Rossi, M.; Pedersen, J.; Schutz, H. *Opt. Eng.* **1994**, *33*, 3556.
(13) Martin, C. *Science* **1994**, *266*, 1961.
(14) Piner, R.; Zhu, J.; Xu, F.; Hong, S.; Mirkin, C. *Science* **1999**, *283*, 661.
(15) Wu, M.; Whitesides, G. *Appl. Phys. Lett.* **2001**, *78*, 2273.
(16) Wu, M.; Paul, K.; Whitesides, G. *Appl. Opt.* **2002**, *41*, 2575.
(17) Hulteen, J.; Van Duyne, R. *J. Vac. Sci. Technol., A* **1995**, *13*, 1553.
(18) Guo, Q.; Teng, X.; Yang, H. *Nano Lett.* **2004**, *4*, 1657.
(19) McLellan, J.; Geissler, M.; Xia, Y. *J. Am. Chem. Soc.* **2004**, *126*, 10830.
(20) Haynes, C.; Van Duyne, R. *J. Phys. Chem. B* **2001**, *105*, 5599.
(21) Burmeister, F.; Schäfle, C.; Matthes, T.; Böhmisch, M.; Boneberg, J.; Leiderer, P. *Langmuir* **1997**, *13*, 2983.
(22) Tormen, M.; Businaro, L.; Altissimo, M.; Romanato, F. *Microelectron. Eng.* **2004**, *73/74*, 535.
(23) Li, Y.; Cai, W.; Duan, G. *Chem. Mater.* **2008**, *20*, 615.
(24) Li, Y.; Naoto, K.; Cai, W. *Coord. Chem. Rev.* **2011**, *255*, 357.
(25) Li, L.; Lu, Y.; Doerr, D.; Alexander, D.; Shi, J.; Li, J. *Nanotechnology* **2004**, *15*, 333.
(26) Zhu, F.; Fan, D.; Zhu, X.; Zhu, J.; Cammarata, R.; Chien, C. *Adv. Mater.* **2004**, *16*, 2155.
(27) Rybczynski, J.; Ebels, U.; Giersig, M. *Colloids Surf., A: Physicochem. Eng. Aspects* **2003**, *219*, 1.
(28) Bartlett, P.; Ghanem, M.; El Hallag, I.; Groot, P.; Zhukov, A. *J. Mater. Chem.* **2003**, *13*, 2596.
(29) Kempa, K.; Kimball, B.; Rybczynski, J.; Huang, Z. *Nano Lett.* **2003**, *3*, 13.
(30) Ji, T.; Lirtsman, V.; Avny, Y.; Davidov, D. *Adv. Mater.* **2001**, *13*, 1253.
(31) Yin, Y.; Lu, Y.; Xia, Y. *J. Am. Chem. Soc.* **2001**, *123*, 771.
(32) Choi, D.; Yu, H.; Jang, S.; Yang, S. *J. Am. Chem. Soc.* **2004**, *126*, 7019.
(33) Xia, Y.; Gates, B.; Yin, Y.; Lu, Y. *Adv. Mater.* **2000**, *12*, 693.
(34) Huang, L.; Yu, Y.; Shen, X.; Li, J.; Shi, B. *Acta Polym. Sin.* **2001**, *4*, 523.
(35) Jiang, P.; Prasad, T.; McFarland, M.; Colvin, V. *Appl. Phys. Lett.* **2006**, *89*, 011908.
(36) Zong, Q.; Xie, X.; Wang, X. *Chem. J. Chin. Univ. Chin* **2004**, *25*, 2363.
(37) Almeida, R.; Goncalves, M.; Portal, S. *J. Non Cryst. Solids* **2004**, *345/346*, 562.
(38) Ye, Y.; LeBlanc, F.; Haché, A.; Truong, V. *Appl. Phys. Lett.* **2001**, *78*, 52.
(39) Ye, Y.; Badilescu, S.; Truong, V.; Rochon, P.; Natansohn, A. *Appl. Phys. Lett.* **2001**, *79*, 872.
(40) Li, X.; Wang, T.; Zhang, J.; Yan, X.; Zhang, X.; Zhu, D. *Langmuir* **2010**, *26*, 2930.
(41) Lu, G.; Li, W.; Yao, J.; Zhang, G.; Yang, B.; Shen, J. *Adv. Mater.* **2002**, *14*, 1049.
(42) Zhu, D.; Li, X.; Zhang, G.; Li, W.; Zhang, X.; Zhang, X.; Wang, T.; Yang, B. *Langmuir* **2010**, *26*, 5172.
(43) Stöber, W.; Fink, A.; Bohn, E. *J. Colloid Interface Sci.* **1968**, *26*, 62.
(44) Yan, X.; Yao, J.; Lu, G.; Li, X.; Zhang, J.; Han, K.; Yang, B. *J. Am. Chem. Soc.* **2005**, *127*, 7688.
(45) Li, X.; Wang, T.; Zhang, J.; Zhu, D.; Zhang, X.; Ning, Y.; Zhang, H.; Yang, B. *ACS Nano* **2010**, *4*, 4350.
(46) Li, W.; Nie, Y.; Zhang, J.; Wang, Z.; Zhu, D.; Lin, Q.; Yang, B.; Wang, Y. *J. Mater. Chem.* **2006**, *16*, 2135.